Research Square

Preprints are preliminary reports that have not undergone peer review.
They should not be considered conclusive, used to inform clinical practice,
or referenced by the media as validated information.

# RNF170 frameshift deletion in Miniature American Shepherd dogs with neuroaxonal dystrophy provides a naturally occurring model for human RNF170 phenotypic spectrum

**Shawna R. Cook**
Purdue University
**Cleo Schwarz**
University of Bern
**Julien Guevar**
AniCura Thun
**Charles-Antoine Assenmacher**
University of Pennsylvania
**Maeve Sheehy**
Purdue University
**Nathan Fanzone**
University of Pennsylvania
**Molly E. Church**
University of Pennsylvania
**Leonardo Murgiano**
University of Pennsylvania
**Margret L. Casal**
University of Pennsylvania
**Vidhya Jagannathan**
University of Bern
**Rodrigo Gutierrez-Quintana**
University of Glasgow
**Mark Lowrie**
Movement Referrals: Independent Veterinary Specialists
**Frank Steffen**
University of Zurich
**Tosso Leeb**
University of Bern
**Kari J. Ekenstedt** ( kje0003@purdue.edu )
Purdue University

**Research Article**

**Keywords:**

**Posted Date:** February 1st, 2024

**DOI:** https://doi.org/10.21203/rs.3.rs-3914204/v1

**License:** This work is licensed under a Creative Commons Attribution 4.0 International License.
Read Full License

**Additional Declarations:** Competing interest reported. The Animal Disease Diagnostic Laboratory at Purdue University (Cook, Sheehy, Ekenstedt) offers a genetic test for RNF170-associated neuroaxonal degeneration. The proceeds of this test are reinvested into Purdue's Canine Genetics Laboratory (a research laboratory), to fund additional research. The remaining authors have no conflicts of interest to declare that are relevant to the content of this article.

# Abstract

Neuroaxonal dystrophy (NAD) is a group of inherited neurodegenerative disorders characterized primarily by the presence of spheroids (swollen axons) throughout the central nervous system. In humans, NAD is heterogeneous, both clinically and genetically. NAD has also been described to naturally occur in large animal models, such as dogs. A newly recognized disorder in Miniature American Shepherd dogs (MAS), consisting of a slowly progressive neurodegenerative syndrome, was diagnosed as NAD via histopathology. Affected dogs were typically young adults and displayed an abnormal gait characterized by pelvic limb weakness and ataxia. A combined GWAS and autozygosity mapping approach, together with whole-genome sequencing, identified the underlying genetic cause as a 1-bp deletion in *RNF170* (*ring finger protein 170*), which perfectly segregates in an autosomal recessive pattern. This deletion is predicted to create a frameshift (XM_038559916.1:c.367delG) and early truncation of the RNF170 protein (XP_038415844.1:(p.Ala123Glnfs*11). A significant LOD score of 9.70 in an extended pedigree confirms the linkage of the deletion variant with the canine phenotype. Several *RNF170* variants have been identified in human patients with analogous clinical syndromes, indicating that this novel MAS NAD serves as an excellent large animal model for equivalent human diseases, particularly since affected dogs demonstrate a relatively long lifespan, which represents an opportunity for therapeutic trials. The age of this canine *RNF170* variant is estimated at approximately 30 years, before the reproductive isolation of the MAS breed. This carries implications for the standard Australian Shepherd, the breed from which MAS were developed.


# 1. Introduction

Neuroaxonal dystrophy (NAD) is a group of rare, inherited neurodegenerative diseases characterized by the presence of swollen axons (spheroids) throughout the central, and rarely peripheral, nervous system (Nardocci and Zorzi 2013). NAD has been described in humans (Cowen and Olmstead 1963) and spontaneously in domestic mammalian species, including dogs (Cork et al. 1983), cats (Carmichael et al. 1993), horses (Adams et al. 1996), cattle (Hanshaw et al. 2015), and mice (Bouley et al. 2006). While all types of NAD share the histopathological hallmark of axonal spheroids and neuronal degeneration, there is a great clinical and genetic heterogeneity within species (Kruer 2013; Hahn et al. 2015).

In humans, multiple types of NAD are differentiated based on the clinical and morphological findings and underlying genetic defects. Many of them are associated with increased iron accumulation in the basal ganglia (globus pallidus and substantia nigra) and are therefore classified as neurodegeneration with brain iron accumulation (NBIA) (Hayflick et al. 2018). The most common types of human NAD encompass pantothenate kinase-associated neurodegeneration (PKAN or NBIA1; OMIM 234200), caused by variants in the *PANK2* gene; early-onset infantile neuroaxonal dystrophy (INAD; OMIM 256600) or NBI2A, caused by variants in *PLA2G6*; mitochondrial kinase-associated neurodegeneration (MPAN or NCBIA4; OMIM 614298), due to variants in *C19orf12*; and β-propeller protein-associated neurodegeneration (BPAN or NBIA5; OMIM 300894) with variants in *WDR45* (Hayflick et al. 2018).

Canine NAD has previously been reported in both mixed breed and purebred dogs, including Rottweiler (Lucot et al. 2018), Spanish Water dog (Hahn et al. 2015), Collie (Clark et al. 1982), Chihuahua (Degl'Innocenti et al. 2017), Jack Russell Terrier (Sacre et al. 1993), Dachshund-cross dog (Pintus et al. 2016), Schnauzer-Beagle cross (Fyfe et al. 2011) and Papillons (Tanaka et al. 2017; Tsuboi et al. 2017). To date, four breed-specific forms have the underlying genetic cause identified. NAD in Papillons, which has a very early age-of-onset, is caused by a missense variant in *PLA2G6*. The homologue of this gene has been associated with human infantile neuroaxonal dystrophy and the affected Papillons were proposed as a valuable animal model for human NAD, especially since these patients demonstrate clinical signs within the first four months of life (Tsuboi et al. 2017). The other known causal variants for canine NAD comprise variants in *tectonin beta-propeller repeat-containing 2* (*TECPR2*) in Spanish Water dogs (Hahn et al. 2015), *vacuolar protein sorting 11* (*VPS11*) in Rottweilers (Lucot et al. 2018), and *mitofusin 2* (*MFN2*) in a colony of Schnauzer-Beagle crosses (Fyfe et al. 2011). The existence of NAD in various dog breeds presents a unique opportunity to uncover novel genes linked to the disease, which could have implications not just for dogs, but also as potential candidates for understanding unexplained human cases.

Here, we report on Miniature American Shepherds (MAS) with a slowly progressive neurodegenerative disorder affecting the gait in young adult dogs primarily characterized by pelvic limb weakness and ataxia. Histopathologically, the syndrome is characterized by the presence of axonal spheroids and tissue changes indicative of neuronal degeneration and secondary gliosis. The aim of this study was to describe the clinical and pathological phenotype together with the identification of the underlying genetic cause.

# 2. Materials and methods

*Ethics statement*

All examinations and animal experiments were carried out after obtaining informed written consent for participation by the owner and in accordance with local laws, regulations, and ethical guidelines. Blood samples or buccal swabs were collected with the approval of the Cantonal Committee for Animal Experiments (Canton of Bern; permits BE 71/19 and BE94/2022) or with ethical approval of Purdue University (IACUC # 1901001840).

*Animal selection, and definition of breed and phenotype*

This study was performed with DNA samples from a total of 937 dogs. MAS dogs represent a relatively young breed that was developed from (standard) Australian Shepherd dogs. MAS dogs were recognized as an independent breed in 2012 by the American Kennel Club and provisionally recognized by the European FCI in 2019. Furthermore, unofficial breed designations, such as Miniature Australian Shepherd or Toy Australian Shepherd have also been used by some breeders. We provide the owner-reported breed assignments of all dogs in our study in Table S1. The 937 dogs consist of 485 MAS, 321 Australian Shepherds, 127 Miniature Australian Shepherds, and 4 Toy Australian Shepherds. Samples originated

either from the College of Veterinary Medicine, Purdue University (n = 151) or the Vetsuisse Biobank at the University of Bern (n = 786).

Each dog was assigned to one of three phenotypic categories. The neurological phenotypes were classified by a board-certified neurologist based on neurological examination, clinical reports, or videos of the dogs submitted by the owners. Twenty-five dogs were classified as 'neurological, clinical signs compatible with NAD' by the presence of hind limb weaknesses with or without ataxia, abnormal gait, scuffing of paws/dragging of digits, and kyphosis. All affected dogs exhibited a pacing/ambling gait (atypical ipsilateral movement of limbs), when gait could be adequately visualized. Six neurological dogs with signs that differed from the above mentioned were classified as 'neurological, other'. The remaining 906 dogs were used as controls. For the majority of the controls, the owners reported their dogs as healthy at the time of sampling. For some of the control dogs, no phenotype information regarding neurological diseases was available. More detailed information on the 937 dogs is compiled in Table S1.

*Clinical examinations*

A proportion of affected dogs were evaluated clinically by board-certified veterinary neurologists (n = 10 out of 23 cases that ultimately were homozygous *del/del* at the discovered deletion variant, *RNF170*:XM_038559916.1:c.367delG, Table S1), with a complete neurological evaluation performed. The remaining 13 cases were variably under the care of general practice veterinarians. Following a call for screening of NAD in the breed, additional affected dogs were submitted to the study but not evaluated in person by a veterinary clinician. In this scenario, owners typically submitted videos of the dogs' gait, and these videos were reviewed by a board-certified neurologist (n = 9 out of 23 *del/del* cases, Table S1). The remaining four *del/del* cases were submitted with clinical descriptions only provided by the owners.

*Pathological examinations*

Necropsy reports were available for two neurologically affected MAS dogs (Case #3/Dog #79 and Case #4/Dog #139, Table S1), which were euthanized at the owner's discretion under the care of their general practitioner veterinarian, due to severely diminished quality of life.

A complete necropsy with harvesting and evaluation of all the major organs, the brain, and the spinal cord, was performed on both cases. The tissues were fixed for 48–72 hours in 10% neutral buffered formalin and routinely trimmed and processed. Paraffin-embedded tissues were sectioned at 4–5 microns and stained with hematoxylin and eosin.

Additional sections of the central nervous system were mounted on charged slides (ProbeOn™ Thermo Fisher Scientific) and were used for immunohistochemistry staining for glial cells, including glial fibrillary acidic protein (GFAP) for astrocytes, and ionized calcium-binding adapter molecule 1 (Iba1) for microglia/macrophages. The immunostaining was performed using the Leica Bond RXm automated platform combined with the Bond Polymer Refine Detection kit (Leica #DS9800). Briefly, after dewaxing and rehydration, sections were pretreated with the epitope retrieval BOND ER1 low pH buffer (Leica

#AR9961) for 20 min at 98°C. Endogenous peroxidase was inactivated with 3% $H_2O_2$ for 10 min at room temperature (RT). Nonspecific tissue-antibody interactions were blocked with Leica PowerVision IHC/ISH Super Blocking solution (PV6122) for 30 min at RT. The same blocking solution also served as diluent for the primary antibody. A rabbit polyclonal primary antibody against GFAP (Agilent (Dako), Z0334) and a rabbit monoclonal primary antibody against Iba1 (WAKO, 019-19741) at a concentration of 1/5000 and 1/1500, respectively, were used and incubated on the slides for 45 min at RT. A biotin-free polymeric IHC detection system consisting of HRP conjugated anti-rabbit was then applied for 25 min at RT. Immunoreactivity was revealed with the diaminobenzidine (DAB) chromogen reaction. Slides were finally counterstained in hematoxylin, dehydrated in an ethanol series, cleared in xylene, and permanently mounted with a resinous mounting medium (Thermo Scientific ClearVue™ coverslip). Normal canine brain and spinal cord sections from a young, unaffected mixed-breed dog were used as positive controls. Negative controls were obtained either by omission of the primary antibodies or replacement with an irrelevant isotype-matched rabbit polyclonal or rat monoclonal antibody.

*DNA extraction and exclusion of* PNPLA8

Genomic DNA was isolated from the EDTA blood samples or buccal swabs with either 1) the Maxwell RSC Whole Blood DNA Kit using a Maxwell RSC instrument (Promega, Dübendorf, Switzerland), 2) the Qiagen Puregene Blood and Tissue kit or the Qiagen DNeasy Blood and Tissue kit (Qiagen, Hilden, Germany) following the manufacturer's protocol, or 3) with a standard phenol-chloroform extraction.

Due to the close relatedness of MAS to Australian Shepherds and the overlap of clinical signs in affected dogs, the previously-published *PNPLA8:XM_005630935.2:c.1169_1170dup* frameshift variant, discovered in Australian Shepherds with hereditary ataxia, OMIA variant ID1470 (Abitbol et al. 2022) was first tested in a very small subset (n = 16) of the total 485 MAS dogs. Specifically, four neurologically affected MAS, five unaffected but obligate carrier MAS, and seven old (9 + years of age when tested), distantly related, phenotypically normal MAS were genotyped, and all dogs were homozygous wildtype at *PNPLA8*:XM_005630935.2:c.1169_1170dup, suggesting this variant was likely not causing the NAD in this breed.

*SNV genotyping*

Genomic DNA from a total of 54 dogs were genotyped on the Illumina CanineHD BeadChips containing 220,853 markers (Neogen, Lincoln, NE, USA) (as designated in Table S1). All SNV positions reported herein correspond to the UU_Cfam_GSD_1.0/CanFam4 assembly.

*GWAS*

GWAS was performed with 54 samples (24 cases and 30 controls). Quality control of the SNV genotype data was performed using PLINK v.1.9 (Chang et al. 2015). SNVs with a minor allele frequency of less than 5% or more than 10% missing genotype data and individuals with a genotyping rate of less than 90% were removed. Additionally, unplaced markers with unknown chromosomal position and mtDNA

markers were excluded. After pruning, 54 dogs and 156,213 markers remained in the analysis and were used for the GWAS using the linear mixed model implemented in the GEMMA software (v0.94.1). The genomic inflation factor in the analysis was 0.98, indicating that the population stratification was appropriately controlled for by the mixed model. Bonferroni correction was used to estimate the genome-wide significance threshold at $p = 0.05/156{,}213 = 3.2 \times 10^{-7}$. Manhattan- and QQ-plots were created using the qqman package in R(Turner 2014; Team 2019). The raw SNV genotype data are available in Supplementary File S1.

*Autozygosity mapping*

The genotype data of 22 dogs that were homozygous for the disease-associated allele at the best associated marker were used for autozygosity mapping. The analysis was done using PLINK v.1.9 (Chang et al. 2015). Markers with missing genotypes in one of the cases were excluded. Additionally, a .tped file with all markers from chromosome 16 was created. Visual inspection of this file in an Excel spreadsheet was performed to exactly determine the shared homozygous haplotype in the 22 cases.

*Whole-genome sequencing and variant filtering*

A PCR-free genomic DNA library was prepared from Case #9/Dog #161 and whole-genome sequencing at 24.8x coverage was performed on an Illumina Novaseq 6000 instrument (Illumina, Zurich, Switzerland). Reads were mapped to the UU_Cfam_GSD_1.0 reference genome assembly and variant calling was performed as described in Jagannathan et al., 2019. SnpEff software (Cingolani et al. 2012) together with NCBI annotation release 106 for the UU_Cfam_GSD_1.0 genome reference assembly was used to predict the functional effects of the called variants. The sequencing data of this single affected dog was compared against 960 control genomes of different breeds to filter for private variants (Table S2).

*PCR and Sanger sequencing*

The candidate variant *RNF170*:XM_038559916.1:c.367delG was genotyped by direct Sanger sequencing of PCR amplicons. The amplification of a 368 bp (or 367 bp in case of the mutant allele) PCR product was performed using the primers 5'-TTTTTCAGCATTGGAGCAGTT-3' (forward) and 5'-TGATGCTTTCTGGATACAAACATT-3' (reverse) and AmpliTaqGold360MasterMix (Thermo Fisher Scientific, Waltham, MA, USA) together with additional 20% of GC enhancer (Thermo Fisher Scientific). Post amplification, the samples were treated with exonuclease I and alkaline phosphatase and subsequently sequenced with ABI BigDye v3.1. PCR amplicons were sequenced with the PCR primers on an ABI 3730 DNA Analyzer (Thermo Fisher Scientific) and the resulting Sanger sequences were analyzed using the Sequencher 5.1 software (GeneCodes, Ann Arbor, MI, USA).

*Post-hoc linkage mapping*

Affected dogs from both Europe and North America were all connected via one large pedigree (Figure S1). A post-hoc LOD score was calculated using dogs with pedigree information and genotypes for

Chr16:23,653,869:delG in LAMP software (Li et al. 2006). Due to the complexity of this large canine pedigree, it was divided into eight smaller families to allow the program to run. The recessive genetic model option was used, and disease prevalence was set at 2%.

*Estimation of age of mutation*

Runs of homozygosity encompassing the identified variant in *RNF170* were identified in PLINK v1.9 (Chang et al. 2015) with default parameters, and linkage map positions across the region were approximated (Wong et al. 2010). The distance from the presumed causal variant and decay of homozygosity in either direction was calculated. The variant was dated using a previously described methodology (Gandolfo et al. 2014) specifically designed for SNP array data from small datasets.

# 3. Results

*Clinical phenotype*

Clinical history of the first proband entailed a two-year-old female intact Miniature American Shepherd with slowly progressive hind limb weakness and incoordination (Case #9/Dog #161, Table S1). Initial signs of weakness were reported to have occurred at around two years of age. Poor performance during dog agility events also developed over time and a “blocked lumbosacral region gait” was reported by the owner. Neurological evaluation identified normal mentation and cranial nerve responses. Behavior was abnormal with excessive anxiety and fear of strangers. Ambulatory paraparesis with hindlimb ataxia was evident. Segmental spinal reflexes were normal. Mild hypermetria (with hyperextension) in the thoracic limbs was also observed. There was no evidence of pain. The integrity of the sensory innervation was difficult to ascertain in light of the dog’s fearful behavior. The neuroanatomic localization was to the T3-L3 spinal cord segments. A multifocal neuroanatomical localization including the T3-L3 spinal cord segments, C1-C5 spinal cord segments (thoracic limbs hypermetria) and forebrain (excessive anxiety) was not excluded. MRI of the brain, spinal cord and CSF analysis only identified a mild coning of the cerebellum in the foramen magnum.

This dog’s sibling also demonstrated ambulatory paraparesis with hindlimb ataxia and was evaluated by the same neurologist (Case #11/Dog #183, Table S1). For this dog, neither anxiety nor thoracic limb hypermetria was evident. Neuroanatomic localization was to the T3-L3 spinal cord segments. The clinical presentation started at a similar age as in the previously examined sibling and was similarly progressive. No MRI was performed on the second dog.

Review of the videos (see Video S1 for an example) of other affected dogs demonstrated that a majority had varying degrees of hind limb weakness and ataxia, together with scuffing of the nails/dragging of digits. Kyphosis and a pacing/ambling gait were commonly reported. A cerebellar gait was also noted in several dogs. A few dogs had a reported change in behavior. Seizures were only reported in one dog, albeit no video footage of the event was available.

Overall, in the present cohort of MAS dogs from a wide international genetic pool, the onset of clinical signs was typically around the second year of age, although this varied somewhat between dogs; this variability, to an extent, depended on the astuteness of the owner's observations. Slowly progressive T3-L3 myelopathy signs were observed as the most common clinical presentation, with possible cervical, cerebellar or forebrain signs also developing. Neither pain nor vestibular signs were reported in affected dogs. Gait abnormalities were always more obvious during the walk compared to faster gaits.

*Histopathological phenotype*

In both necropsied cases (Case #3/Dog #79 and Case #4/Dog #139, Table S1) the evaluation of the brain and spinal cord showed widespread and bilateral neuroaxonal degeneration throughout the gray and white matter with the lateral cuneate nuclei in the brainstem being most severely affected (Fig. 1a). The neuroaxonal degeneration consisted of variable numbers of large, swollen and hypereosinophilic axons (spheroids), dilated myelin sheaths, degenerated or dead neurons, and mixed gliosis (Fig. 1a, inset). The gliosis was further highlighted by GFAP and Iba1 immunohistochemistry stains (Fig. 1b-c), which showed increased density of glial cells in the affected regions and occasional formation of glial cell aggregates. No other significant changes were seen in any of the organs evaluated.

*Genetic investigation*

As the clinical and pathological examinations were highly suggestive of an inherited disease, we compiled pedigree information on the available cases, ultimately generating a pedigree spanning both European and North American cases (Figure S1). The pedigree was compatible with a monogenic autosomal recessive mode of inheritance. For the identification of the causal genetic variant, we initially performed a GWAS with 24 dogs classified as 'neurological, clinical signs compatible with NAD' and 30 unaffected controls. This analysis yielded a clear association signal on chromosome 16 exceeding the Bonferroni significance threshold ($p = 3.25 \times 10^{-8}$; Fig. 2a). Autozygosity mapping revealed that 22 of the GWAS-cases shared an identical ~ 2.69 Mb homozygous haplotype. The first heterozygous markers on either side of the homozygous region defined an exact critical interval for the NAD variant, Chr16:21,289,584–23,975,245 (all positions reported in UU_Cfam_GSD_1.0/CanFam4) (Fig. 2b, Table S3).

We sequenced the genome of one case (Case #9/Dog #161, Table S1) and compared the data to 960 control genomes (Table 1, Table S2). Variant filtering revealed only two private homozygous variants in the critical interval. One was an intronic SNV that was not further investigated. The remaining variant was a 1-bp deletion in the *RNF170* (*ring finger protein 170*) gene and can be designated as Chr16:23,653,869:delG (UU_Cfam_GSD_1.0 assembly), located in the critical interval (Fig. 2c). This frameshift variant, XM_038559916.1:c.367delG, is predicted to lead to a truncation of 48% of the wild type open reading frame, XP_038415844.1:(p.Ala123Glnfs*11) (Figure S2). The Chr16:23,653,869:delG variant is also absent from the most recently published Dog10K dataset comprising 2075 genetically diverse canids (Meadows et al. 2023).

Table 1
Results of variant filtering in an NAD affected MAS against 960 control genomes.

| Filtering step | Homozygous variants |
|---|---|
| all variants in the affected MAS dog | 2,428,434 |
| private variants in whole genome | 434 |
| protein-changing private variants in whole genome | 2 |
| private variants in the critical interval | 2 |
| protein-changing private variants in the critical interval | 1 |
| in functional candidate genes for similar phenotypes in other species | 1 |

We next genotyped a large cohort of 937 dogs, including the original GWAS cases, for the *RNF170* single base deletion. This revealed 27 dogs as homozygous for the deletion, 98 heterozygous carriers and 813 dogs homozygous for the wildtype allele. Twenty-three of the 27 homozygous mutant dogs showed clinical signs compatible with NAD (~ 85%). The remaining four dogs did not show any signs of NAD. However, these four discordant dogs were relatively young (6, 19, 27 and 43 months of age, respectively). The cohort also comprised six dogs with neurological signs differing from the NAD phenotype. These dogs were either homozygous (n = 5) or heterozygous (n = 1) for the wildtype allele. Two additional neurological dogs whose clinical signs were indistinguishable from the other NAD cases also did not carry the mutant *RNF170* allele (Table 2).

Table 2
Association of the genotypes at *RNF170*:c.367delG variant with phenotype in 937 dogs.

| Phenotype group | *G/G* | *G/del* | *del/del* |
|---|---|---|---|
| Neurological, clinical signs compatible with NAD (n = 25) | 2 | - | 23 |
| Neurological, other (n = 6) | 5 | 1 | - |
| Controls, Miniature/Toy American/Australian Shepherd dogs (n = 586) | 485 | 97 | 4[a] |
| Controls, Australian Shepherd dogs, (n = 320) | 320 | - | - |

[a]These four dogs were all younger than 43 months at the time of writing.

Post-hoc linkage mapping calculated a LOD score of 9.70 for the identified *RNF170* deletion in an extended pedigree (Figure S1), demonstrating significant linkage between the genotype and NAD phenotype.

Estimation of the age of the mutation indicated that the variant arose approximately 13.7 generations ago (95% CI: 2.9–25.1), under a “correlated genealogy” model (a model allowing for more than one

common/shared ancestor, which is nearly always the case in purebred dogs). Given a generation interval of two years, the mutation event is predicted to have occurred ~ 27.4 years ago.

# 4. Discussion

In a highly unique situation, three different research laboratories (Purdue University, University of Bern, and University of Pennsylvania) all independently identified the *RNF170* variant in NAD affected dogs using slightly different approaches. After realizing that all three groups worked on the same disease and a related set of dogs, we combined the data to produce the present comprehensive report characterizing neuroaxonal dystrophy in the Miniature American Shepherd, a new autosomal recessively inherited canine neurologic disease.

Histopathologic examination of affected dogs demonstrated abundant large, irregularly-shaped spheroids, particularly in the brainstem, which is consistent with neuroaxonal dystrophies (Sisó et al. 2006). Although these spheroids can be found throughout the brain, they are usually found in the gray matter of brainstem nuclei and spinal cord (dorsal column nuclei), which is considered the characteristic distribution for NAD (Sisó et al. 2006; Hanshaw et al. 2015). The neurohistopathological diagnosis of NAD corroborates the genetic findings in these dogs. Given the present findings, together with the context of previously existing canine NAD diseases, it is clear that the development of a global pathology consortium to gather the pathology reports of NAD-positive dogs would be beneficial; this would allow for the creation of a canine NAD pathology repository, which would benefit not only veterinary medicine and canine patients, but also human medicine, by defining excellent, naturally-occurring, large animal models.

A hypothesis-free genetic analysis identified a frameshift deletion in the *RNF170* gene as the most likely causal variant. *RNF170* encodes an E3 ubiquitin ligase located in the endoplasmic reticulum membrane (ER) that mediates ubiquitination-dependent degradation of inositol 1,4,5-triphosphate receptors (IP3Rs) via the ER-associated protein degradation (ERAD) pathway (Vembar and Brodsky 2008; Lu et al. 2011). Activation of IP3Rs leads to $Ca^{2+}$ efflux from the ER into the cytoplasm. After activation, RNF170 is recruited by the ERLIN1/ERLIN2 complex and enables the proteasomal degradation of IP3 receptors, thus having an impact on $Ca^{2+}$ homeostasis (Lu et al. 2011; Gao and Wojcikiewicz 2020). Dysregulation of $Ca^{2+}$ homeostasis and signaling have been implicated in various neurodegenerative diseases such as Alzheimer's and Huntington's disease (Tong et al. 2018; Czeredys 2020). Variants in key genes encoding components of the ERAD pathway, such as in *ERLIN1*, *ERLIN2* or *RNF170* have been reported to cause hereditary spastic paraplegia (HSP) in humans (MIM #615681, MIM#611225, MIM#619686) (Wakil et al. 2013; Novarino et al. 2014; Rydning et al. 2018; Wagner et al. 2019). Human *RNF170* variants are further associated with autosomal dominant sensory ataxia (SNAX1) (MIM#608984) (Moeller et al. 2008; Valdmanis et al. 2011).

HSP comprises a genetically and clinically heterogenous group of rare, neurodegenerative motor neuron disorders characterized by variable bilateral progressive weakness, stiffness, and spasticity in the limbs (Fink 2013). More than 80 genes have been associated with HSP (Elsayed et al. 2021); and the clinical

and genetic heterogeneity can make the diagnosis challenging (Chouery et al. 2022). To date, seven different variants in *RNF170* were identified in human patients with early to adolescent-onset HSP (Wagner et al. 2019; de Sainte Agathe et al. 2021; Chouery et al. 2022; Fu et al. 2023). Even among patients with known *RNF170* variants underlying their HSP, the clinical picture can vary. For example, in a group of nine people, five had normal cranium and cervical spine on MRI, while two had cerebellar atrophy; in the same group, five patients had delayed motor development while four developed age appropriately (Wagner et al. 2019).

SNAX1 (hereditary sensory ataxia 1) in humans is caused by a heterozygous *RNF170* variant (R199C), and affected individuals experience adult onset, slowly-progressive gait ataxia and clumsiness, together with distal sensory loss (Valdmanis et al. 2011; Cortese et al. 2020). Interestingly, however, the SNAX1 *RNF170*:p.R199C variant does not affect the ubiquitination of activated IP3R (Wright et al. 2015). Given this, and the fact that heterozygous carriers of nonsense variants in *RNF170* have been shown to be unaffected (Kim et al. 2015; Wright et al. 2015; Wagner et al. 2019), it has been hypothesized that the age-dependent gait problems of human SNAX1 patients might be due to toxic gain-of-function of mutant RNF170 proteins, independent from endogenous RNF170 function (Cortese et al. 2020). Interestingly, one dog in the present study (Dog #515, Table S1) phenotyped as “neurological, other” is a heterozygous carrier of the of the *RNF170* deletion. It seems unlikely that this dog’s clinical signs are related to its carrier status, given the numerous other heterozygous dogs living to older age with no neurological issues, and the relatively young age-of-onset of this dog’s clinical signs (~ 1 year). More likely, this suggests that one or more additional variants underlying neurological conditions remain to be discovered in the MAS.

A murine model (*Rnf170*$^{-/-}$) also demonstrated later onset (~ 12 months) and progression of clinical signs over time (Kim et al. 2015). In mice, the *Rnf170*$^{-/-}$ gait abnormality was suggested to be specifically associated with inter-limb coupling and step sequence mechanisms, rather than a secondary effect.

The naturally occurring MAS canine model of NAD in the present study clearly demonstrates autosomal recessive inheritance, together with a predicted loss-of-function variant, thus mimicking human *RNF170*-related HSP conditions. However, clinically, the affected dogs may share more similarities with the typical presentation of *RNF170* SNAX1 in humans, including post-adolescent age of onset. Although not fatal per se, affected MAS dogs eventually develop more severe disabilities, leading to poor quality of life and frequent euthanasia. HSPs in people have historically been classified as “pure” and “complex/complicated” forms, with the former characterized primarily by spasticity without other significant findings and the latter being associated with additional features, such as seizures, neuropathies, short stature, visual abnormalities, and others (Blackstone 2018). Today, such clinical classifications have been largely superseded by genetic classifications (Blackstone 2018). Taken together, *RNF170*-related NAD in MAS provides an excellent spontaneous large animal model for HSPs and SNAX1 in people.

Long-term outcome information for NAD-affected MAS is currently limited, as many of these dogs are still alive. The T3-L3 myelopathy was the most evident finding; whether or not the thoracic limb hypermetria and behavioral changes (and reported seizures in a single case) are NAD-related is unclear, but could suggest these dogs experience a more “complex/complicated” phenotype rather than a “pure” form of the disease. This highlights the need for further studies over longer time frames that include clinical evaluation of NAD homozygous dogs to understand the complete relationship between age, clinical status, and the now-known genetic status. When possible, definition of the phenotype would be further enhanced by electrodiagnostic testing. Crucially, the lifespan of NAD-affected MAS is not markedly decreased, representing an opportunity for therapeutic trials in this large animal model. There is currently no treatment for NAD in affected dogs; the findings in the present study provide a foundation for potential future studies investigating treatment options.

While the association of the genotypes at the *RNF170*:c.367delG variant with the NAD phenotype was very strong, it was not perfect. We observed a total of six discordant dogs in a cohort of 937 dogs. Four dogs that were homozygous for the deletion did not show clinical signs. Two of them were younger than two years of age and thus below the typical age of onset for NAD in our cohort. The other two were 27 and 43 months old and thus of an age when clinical signs were noticeable in most of the other cases. We speculate that the NAD phenotype in these two dogs was particularly mild or had a delayed age of onset. This underscores the importance of genetic testing in order to stop further propagation of the disease. We also cannot exclude the possibility of incomplete penetrance. Two other dogs showed clinical signs indistinguishable from NAD but had a wildtype genotype. This most likely points to genetic heterogeneity and the potential existence of additional inherited, degenerative neurological diseases in the Miniature American Shepherd.

We observed the mutant allele only in Miniature American Shepherds and related breeds, but not in standard Australian Shepherds. This may indicate that the deleterious allele arose only recently after the separation of the populations. Estimation of the age of the deletion variant predicts the mutation event occurred approximately 27 years ago, or around the early- to mid-1990s. The first parent breed club and registry for North American MAS was formed in 1990 (https://mascusa.org/breed/history, accessed 20 Jan 2024) and, at least in the American Kennel Club, the MAS stud book is still open, meaning that standard Australian Shepherds can still be bred into MAS lines. Therefore, we cannot definitively rule-out the presence/absence of this deletion in the Australian Shepherd breed; instead, we recommend confirmation by testing additional representative standard Australian Shepherd dogs from different countries before a general all-clear signal is given to this breed.

Importantly, the disease allele frequency specifically in the MAS control cohort was found at 8.3% (this does not include the standard Australian Shepherds), which corresponds to a carrier frequency of 16.6%. While these numbers may overestimate the true frequencies due to biased sampling for our study, they clearly warrant genetic testing and a targeted breeding program to avoid future carrier x carrier matings for these dogs.

In conclusion, the clinical and pathologic picture presented by MAS affected with *RNF170*-related NAD is strikingly similar to the phenotypic spectrum (HSP, SNAX1) seen in human patients with *RNF170* variants. Thus, NAD in the MAS represents an excellent, spontaneously occurring large animal model for *RNF170* conditions in people.

# Declarations


### Funding:

Partial funding for KJE was provided by the Office of the Director, National Institutes of Health (NIH) under award number K01OD027051. The Van Sloun Fund for Canine Genetic Research contributed to the work carried out by LM and MLC.


### Data availability:

Dog SNV array data are given in File S1. Whole-genome sequence from Case #9/Dog #161 is publicly available under study accession number PRJEB16012 and sample accession number SAMEA112638856. All other accessions are given in Table S2.

### Ethics declarations

*Conflict of interest:* The Animal Disease Diagnostic Laboratory at Purdue University (Cook, Sheehy, Ekenstedt) offers a genetic testy for *RNF170*-associated neuroaxonal degeneration. The proceeds of this test are reinvested into Purdue's Canine Genetics Laboratory (a research laboratory), to fund additional research. The remaining authors have no conflicts of interest to declare that are relevant to the content of this article.

*Ethical approval:* Sample collection was ethically approved by Purdue University's Institutional Animal Care and Use Committee (IACUC) (#1901001840) and the Cantonal Committee for Animal Experiments (Canton of Bern; permit BE 71/19). All dogs in this study were privately owned pet dogs.

*Consent to participate:* All dog owners provided written consent when donating samples from their dog(s).

*Consent for publication:* Written consent for publication was obtained and is on record from the owner of the dog shown in the Supplemental Video.


### Acknowledgements:

The authors are grateful to all dog owners across who donated samples and participated in the study. We thank the Next-Generation Sequencing Platform of the University of Bern for performing the high-throughput sequencing experiments and the Interfaculty Bioinformatics Unit of the University of Bern for providing high-performance computing infrastructure. We acknowledge the DBVDC consortium, the

Dog10K genomes project and all researchers who deposited dog or wolf whole-genome sequencing data into public databases.

**Contributions:**

Conceptualization: SRC, TL, KJE

Performed laboratory experiments: SRC, CS, MS

Performed clinical evaluations of patients: JG, RQG, ML, FS

Performed pathological evaluations of patients: CAA, NF, MEC

Analyzed data: SRC, CS, LM

Visualization: SRC, CS, CAA, MS, TL, KJE

Data curation: SRC, VJ

Writing - original draft: SRC, CS, TL, KJE

Writing - editing and review: SRC, CS, JG, CAA, MS, NF, MEC, LM, MLC, VJ, RGQ, ML, FS, TL, KJE

Supervision: MLC, TL, KJE

Funding acquisition: LM, MLC, KJE

# References

1. Abitbol M, Jagannathan V, Laurent N, et al (2022) A PNPLA8 frameshift variant in Australian shepherd dogs with hereditary ataxia. Anim Genet 53:709–712. https://doi.org/10.1111/age.13245
2. Adams AP, Collatos C, Fuentealba C, et al (1996) Neuroaxonal dystrophy in a two-year-old quarter horse filly. Can Vet J 37:43–44
3. Blackstone C (2018) Hereditary spastic paraplegia, 1st edn. Elsevier B.V.
4. Bouley DM, McIntire JJ, Harris BT, et al (2006) Spontaneous Murine Neuroaxonal Dystrophy: a Model of Infantile Neuroaxonal Dystrophy. J Comp Pathol 134:161–170. https://doi.org/10.1016/j.jcpa.2005.10.002
5. Carmichael KP, Howerth EW, Oliver JE, Klappenbach K (1993) Neuroaxonal Dystrophy in a Group of Related Cats. J Vet Diagnostic Investig 5:585–590. https://doi.org/10.1177/104063879300500414
6. Chang CC, Chow CC, Tellier LCAM, et al (2015) Second-generation PLINK: Rising to the challenge of larger and richer datasets. Gigascience 4:1–16. https://doi.org/10.1186/s13742-015-0047-8
7. Chouery E, Mehawej C, Megarbane A (2022) A novel homozygous variant in RNF170 causes hereditary spastic paraplegia: a case report and review of the literature. Neurogenetics 23:85–90.

https://doi.org/10.1007/s10048-022-00685-6

8. Clark RG, Hartley WJ, Burgess GS, et al (1982) Suspected inherited cerebellar neuroaxonal dystrophy in collie sheep dogs. N Z Vet J 30:102–103. https://doi.org/10.1080/00480169.1982.34897
9. Cork LC, Troncoso JC, Price DL, et al (1983) Canine Neuroaxonal Dystrophy. J Neuropathol Exp Neurol 42:286–296. https://doi.org/https://doi.org/10.1097/00005072-198305000-00006
10. Cortese A, Callegari I, Curro R, et al (2020) Mutation in RNF170 causes sensory ataxic neuropathy with vestibular areflexia: A CANVAS mimic. J Neurol Neurosurg Psychiatry 91:1237–1238. https://doi.org/10.1136/jnnp-2020-323719
11. Cowen D, Olmstead E V (1963) Infantile Neuroaxonal Dystrophy. J Neuropathol Exp Neurol 22:175–236. https://doi.org/https://doi.org/10.1097/00005072-196304000-00001
12. Czeredys M (2020) Dysregulation of Neuronal Calcium Signaling via Store-Operated Channels in Huntington's Disease. Front Cell Dev Biol 8:. https://doi.org/10.3389/fcell.2020.611735
13. de Sainte Agathe JM, Mercier S, Mahé JY, et al (2021) RNF170-Related Hereditary Spastic Paraplegia: Confirmation by a Novel Mutation. Mov Disord 36:771–774. https://doi.org/10.1002/mds.28371
14. Degl'Innocenti S, Asiag N, Zeira O, et al (2017) Neuroaxonal Dystrophy and Cavitating Leukoencephalopathy of Chihuahua Dogs. Vet Pathol 54:832–837. https://doi.org/10.1177/0300985817712557
15. Elsayed LEO, Eltazi IZ, Ahmed AE, Stevanin G (2021) Insights into Clinical, Genetic, and Pathological Aspects of Hereditary Spastic Paraplegias: A Comprehensive Overview. Front Mol Biosci 8:. https://doi.org/10.3389/fmolb.2021.690899
16. Fink JK (2013) Hereditary spastic paraplegia: Clinico-pathologic features and emerging molecular mechanisms. Acta Neuropathol 126:307–328. https://doi.org/10.1007/s00401-013-1115-8
17. Fu JX, Wei Q, Chen YL, Li HF (2023) Novel stop-gain RNF170 variation detected in a Chinese family with adolescent-onset hereditary spastic paraplegia. Clin Genet 103:87–92. https://doi.org/10.1111/cge.14219
18. Fyfe JC, Al-Tamimi RA, Liu J, et al (2011) A novel mitofusin 2 mutation causes canine fetal-onset neuroaxonal dystrophy. Neurogenetics 12:223–232. https://doi.org/10.1007/s10048-011-0285-6
19. Gandolfo LC, Bahlo M, Speed TP (2014) Dating rare mutations from small samples with dense marker data. Genetics 197:1315–1327. https://doi.org/10.1534/genetics.114.164616
20. Gao X, Wojcikiewicz RJH (2020) The emerging link between IP3 receptor turnover and Hereditary Spastic Paraplegia. Cell Calcium 86:2019–2020. https://doi.org/10.1016/j.ceca.2019.102142
21. Hahn K, Rohdin C, Jagannathan V, et al (2015) TECPR2 associated neuroaxonal dystrophy in Spanish water dogs. PLoS One 10:1–18. https://doi.org/10.1371/journal.pone.0141824
22. Hanshaw DM, Finnie JW, Manavis J, Kessell AE (2015) Axonal Spheroid Accumulation In the Brainstem and Spinal Cord of A Young Angus Cow with Ataxia. Aust Vet J 93:283–286. https://doi.org/10.1111/avj.12346

23. Hayflick SJ, Kurian MA, Hogarth P (2018) Neurodegeneration with brain iron accumulation. Handb Clin Neurol 147:293–305. https://doi.org/10.1016/B978-0-444-63233-3.00019-1
24. Kim Y, Kim SH, Kim KH, et al (2015) Age-dependent gait abnormalities in mice lacking the Rnf170 gene linked to human autosomal-dominant sensory ataxia. Hum Mol Genet 24:7196–7206. https://doi.org/10.1093/hmg/ddv417
25. Kruer MC (2013) The Neuropathology of Neurodegeneration with Brain Iron Accumulation, 1st edn. Elsevier Inc.
26. Li M, Boehnke M, Abecasis GR (2006) Efficient study designs for test of genetic association using sibship data and unrelated cases and controls. Am J Hum Genet 78:778–792. https://doi.org/10.1086/503711
27. Lu JP, Wang Y, Sliter DA, et al (2011) RNF170 protein, an endoplasmic reticulum membrane ubiquitin ligase, mediates inositol 1,4,5-trisphosphate receptor ubiquitination and degradation. J Biol Chem 286:24426–24433. https://doi.org/10.1074/jbc.M111.251983
28. Lucot KL, Dickinson PJ, Finno CJ, et al (2018) A missense mutation in the vacuolar protein sorting 11 (VPS11) gene is associated with neuroaxonal dystrophy in rottweiler dogs. G3 Genes, Genomes, Genet 8:2773–2780. https://doi.org/10.1534/g3.118.200376
29. Meadows JRS, Kidd JM, Wang GD, et al (2023) Genome sequencing of 2000 canids by the Dog10K consortium advances the understanding of demography, genome function and architecture. Genome Biol 24:. https://doi.org/10.1186/s13059-023-03023-7
30. Moeller JJ, Macaulay RJB, Valdmanis PN, et al (2008) Autosomal dominant sensory ataxia: A neuroaxonal dystrophy. Acta Neuropathol 116:331–336. https://doi.org/10.1007/s00401-008-0362-6
31. Nardocci N, Zorzi G (2013) Axonal dystrophies, 1st edn. Elsevier B.V.
32. Novarino G, Fenstermaker AG, Zaki MS, et al (2014) Exome sequencing links corticospinal motor neuron disease to common neurodegenerative disorders. Science (80- ) 343:506–511. https://doi.org/10.1126/science.1247363
33. Pintus D, Cancedda MG, Macciocu S, et al (2016) Pathological findings in a Dachshund-cross dog with neuroaxonal dystrophy. Acta Vet Scand 58:1–7. https://doi.org/10.1186/s13028-016-0218-3
34. Rydning SL, Dudesek A, Rimmele F, et al (2018) A novel heterozygous variant in ERLIN2 causes autosomal dominant pure hereditary spastic paraplegia. Eur J Neurol 25:943–948. https://doi.org/10.1111/ene.13625
35. Sacre B, Cummings J, Delahunta A (1993) Neuroaxonal dystrophy in a Jack Russell terrier pup resembling human infantile neuroaxonal dystrophy. Cornell Vet 83:133–142
36. Sisó S, Hanzlíček D, Fluehmann G, et al (2006) Neurodegenerative diseases in domestic animals: A comparative review. Vet J 171:20–38. https://doi.org/10.1016/j.tvjl.2004.08.015
37. Tanaka M, Yamaguchi S, Akiyoshi H, et al (2017) Ultrastructural features of canine neuroaxonal dystrophy in a Papillon dog. J Vet Med Sci 79:1927–1930. https://doi.org/10.1292/jvms.17-0487

38. Team RC (2019) R: A language and environment for statistical computing. R Foundation for Statistical Computing, Vienna, Austria. URL: https://www.R-project.org/
39. Tong BCK, Wu AJ, Li M, Cheung KH (2018) Calcium signaling in Alzheimer's disease & therapies. Biochim Biophys Acta - Mol Cell Res 1865:1745–1760. https://doi.org/10.1016/j.bbamcr.2018.07.018
40. Tsuboi M, Watanabe M, Nibe K, et al (2017) Identification of the PLA2G6 c.1579G>A missense mutation in papillon dog neuroaxonal dystrophy using whole exome sequencing analysis. PLoS One 12:1–17. https://doi.org/10.1371/journal.pone.0169002
41. Turner SD (2014) qqman: an R package for visualizing GWAS results using Q-Q and manhattan plots. bioRxiv 81:559–575. https://doi.org/https://doi.org/10.1101/005165
42. Valdmanis PN, Dupré N, Lachance M, et al (2011) A mutation in the RNF170 gene causes autosomal dominant sensory ataxia. Brain 134:602–607. https://doi.org/10.1093/brain/awq329
43. Vembar SS, Brodsky JL (2008) One step at a time: Endoplasmic reticulum-associated degradation. Nat Rev Mol Cell Biol 9:944–957. https://doi.org/10.1038/nrm2546
44. Wagner M, Osborn DPS, Gehweiler I, et al (2019) Bi-allelic variants in RNF170 are associated with hereditary spastic paraplegia. Nat Commun 10:1–13. https://doi.org/10.1038/s41467-019-12620-9
45. Wakil S, Bohlega S, Hagos S, et al (2013) A novel splice site mutation in ERLIN2 causes hereditary spastic paraplegia in a Saudi family. Eur J Med Genet 56:43–45. https://doi.org/https://doi.org/10.1016/j.ejmg.2012.10.003
46. Wong AK, Ruhe AL, Dumont BL, et al (2010) A comprehensive linkage map of the dog genome. Genetics 184:595–605. https://doi.org/10.1534/genetics.109.106831
47. Wright FA, Lu JP, Sliter DA, et al (2015) A point mutation in the ubiquitin ligase RNF170 that causes autosomal dominant sensory ataxia destabilizes the protein and impairs inositol 1,4,5-trisphosphate receptor-mediated Ca2+ signaling. J Biol Chem 290:13948–13957. https://doi.org/10.1074/jbc.M115.655043

# Figures

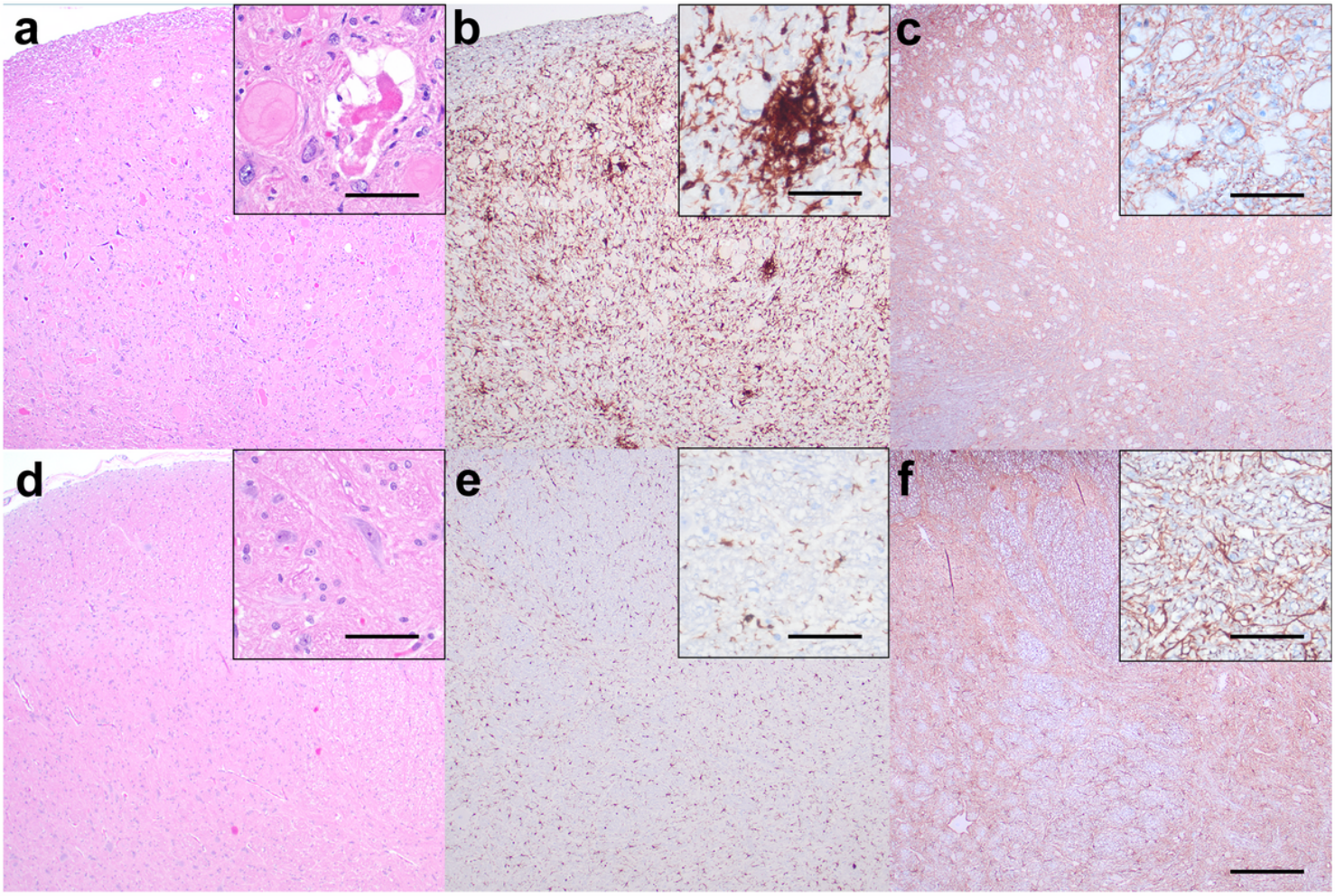


**Figure 1**

**Central nervous system pathology of affected dogs.** Widespread neuroaxonal degeneration and gliosis are observed. **a.** Brainstem, at the level of the lateral cuneate nucleus. The neuroparenchyma demonstrates high numbers of degenerated axons and spheroids along with increased glial cells and dead neurons (inset). Hematoxylin and eosin. **b.** and **c.** Immunohistochemistry for IBA-1 (**b.**) confirms the marked increase in density of microglial cells in the affected regions with formation of Iba-1 positive cell aggregates (**b,** inset). Immunohistochemistry for GFAP (**c.**) only shows a modest increase in astrocytes. Controls (**d-f**) obtained from a young, unaffected, intact male mixed-breed dog. 4x scale bar: 150 micrometers; insets: 40x, scale bar: 60 micrometers.

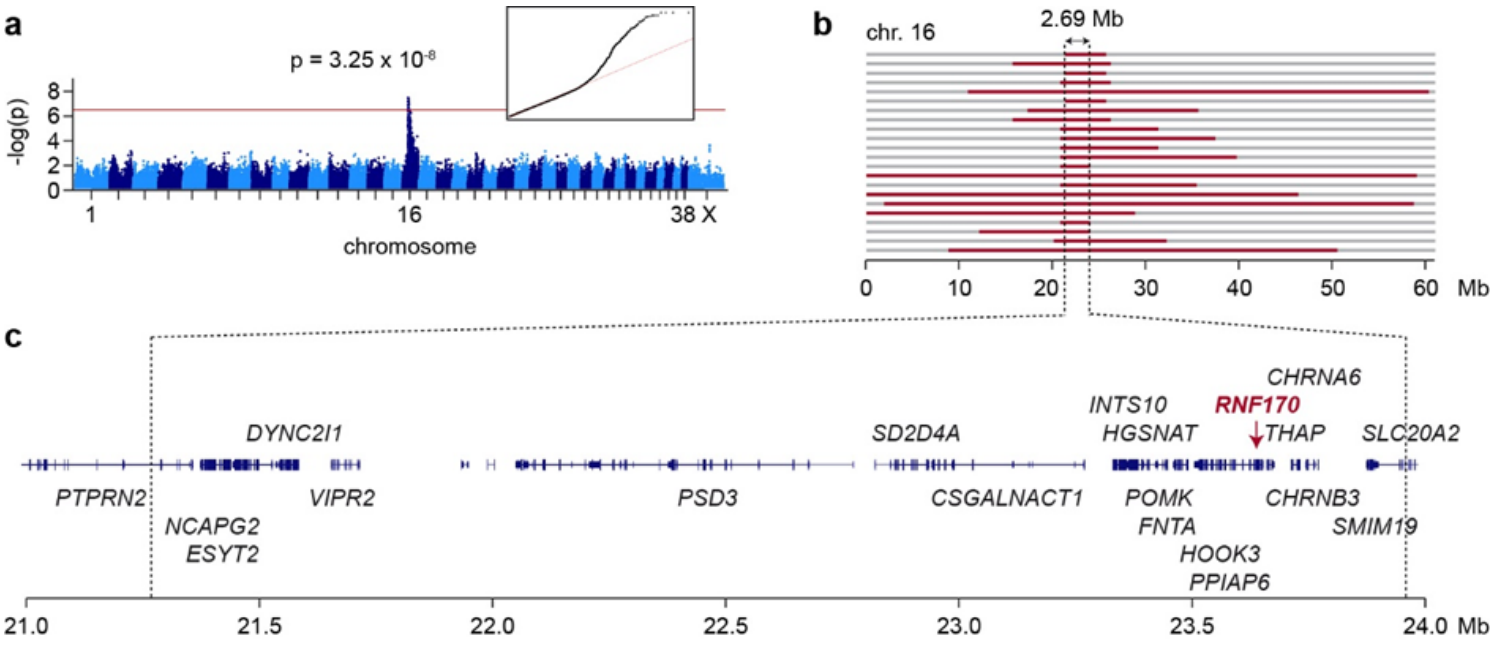


**Figure 2**

Mapping of the MAS NAD locus. **a** Manhattan plot of a GWAS using 24 neurological dogs and 30 controls showed a clear association signal on chromosome 16 with the best associated marker at 21,740,477 bp. The inset shows the QQ-plot. **b** Autozygosity mapping in 22 NAD cases. Each horizontal line indicates the genotypes on chromosome 16 for one dog. Identical homozygous haplotypes are indicated in red. The shared segment defines the critical interval. **c** NCBI annotation release 106 lists 20 genes in the critical interval. Additionally annotated LOCs are not shown. The *RNF170* gene is highlighted in red.

# Supplementary Files

This is a list of supplementary files associated with this preprint. Click to download.

- FigureS1.png
- FigureS2.docx
- FileS1SNVgenotypesMAS.zip
- TableS1.xlsx
- TableS2PublicGenomes.xlsx
- TableS3HomozygosityvisualChr1622cases.xlsx
- VideoS1.mp4